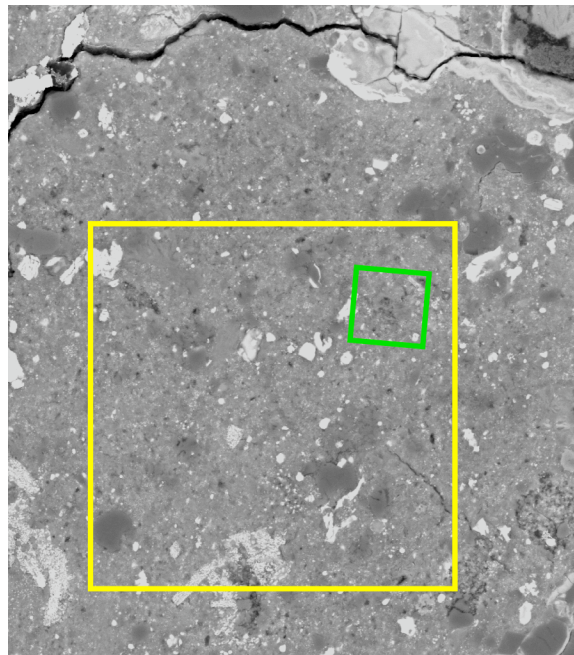


**AN OXYGEN-18 RICH PRESOLAR SILICATE GRAIN FROM THE ACFER 094 METEORITE: A NANOSIMS AND TOF-SIMS STUDY.** F. J. Stadermann<sup>1</sup>, C. Floss<sup>1</sup>, P. A. Bland<sup>2</sup>, E. P. Vicenzi<sup>3</sup>, and D. Rost<sup>3</sup>, <sup>1</sup>Laboratory for Space Sciences and Department of Physics, CB 1105, Washington University, 1 Brookings Drive, St. Louis, MO 63130, USA, <sup>2</sup>Department of Earth Science and Engineering, Imperial College London, South Kensington Campus, London SW7 2AZ, U.K., <sup>3</sup>Department of Mineral Sciences, National Museum of Natural History, Smithsonian Institution, Washington, DC 20560, USA.

**Introduction:** The Acfer 094 meteorite is a primitive carbonaceous chondrite with an unusually high concentration of presolar grains [1-4]. The presolar components of this meteorite's matrix have been identified on the basis of their highly anomalous O isotopic compositions and recent advances in microanalytical technology, most notably the development of the NanoSIMS [1, 3, 4].

In an initially unrelated study [5], we used the NanoSIMS to determine the O isotopic variations in small Ca-Al rich inclusions (micro-CAIs) that were identified in the matrix of Acfer 094 by time-of-flight secondary ion mass spectrometry (ToF-SIMS) imaging. Here we report on the accidental discovery of an <sup>18</sup>O-rich presolar grain during the course of these measurements. Since the area of the presolar grain was previously analyzed by ToF-SIMS, we have correlated elemental and isotopic data to aid in the mineralogical identification of the particle.

**Experimental:** A polished thin section of the Acfer 094 meteorite was initially characterized by electron microscopy as shown in Figure 1. A  $\sim 50 \times 50 \mu\text{m}^2$  area of the matrix was then chosen for a detailed ToF-SIMS elemental study at the Smithsonian Institution. The ToF-SIMS measurements were done with a pulsed 25 kV Ga<sup>+</sup> primary ion beam with a spatial resolution of  $\sim 300$  nm. Complete mass spectra were collected for every pixel in a  $256 \times 256$  array. Several small regions with micro-CAIs were identified on the basis of the ToF-SIMS data and selected for subsequent isotopic imaging studies with the Washington University NanoSIMS. Those measurements were made by rastering a 100 nm Cs<sup>+</sup> primary ion beam across  $7 \times 7$  to  $20 \times 20 \mu\text{m}^2$  areas in  $256^2$  or  $512^2$  pixels and detecting secondary electrons (SE), <sup>16</sup>O<sup>-</sup>, <sup>17</sup>O<sup>-</sup>, <sup>18</sup>O<sup>-</sup>, and <sup>27</sup>Al<sup>-</sup> at high mass resolution. A total of  $650 \mu\text{m}^2$  was studied by NanoSIMS isotope imaging, entirely within the  $2500 \mu\text{m}^2$  area that was previously analyzed by ToF-SIMS (see Figure 1). An additional NanoSIMS measurement was made on a large ( $\sim 50 \mu\text{m}$ ) CAI elsewhere in Acfer 094. The O isotopic compositions of regions of interest inside the raster areas were calculated following standardized routines [e.g., 6] and by using the bulk matrix as an internal standard. All  $\delta$ -values are thus matrix-normalized.



**Figure 1.** Backscattered electron image of the analyzed area in the matrix of Acfer 094. The  $50 \times 50 \mu\text{m}^2$  area of the ToF-SIMS measurements is shown in yellow. The presolar grain was found in the NanoSIMS analysis of the  $10 \times 10 \mu\text{m}^2$  area shown in green.

**Results:** As expected [7], the analysis of the large CAI showed a <sup>16</sup>O-rich composition with  $\delta^{17,18}\text{O}$  around -40‰, while the analyzed micro-CAIs have varying O isotopic compositions [5]. Since the NanoSIMS isotopic measurements were made in imaging mode, we could not fail to notice a presolar grain in one of the analyses. The area with both the CAI and the presolar grain is shown in Figure 2. Note that image smoothing of the false color image leads to an increase in the apparent size and a dilution of the composition of small features, i.e., the presolar grain. This level of image smoothing, however, is required for the analysis of the CAI. A more detailed data analysis of the area shows that the presolar grain has a diameter of 250 nm. Its isotopic composition is  $^{18}\text{O}/^{16}\text{O} = (9.52 \pm 0.12) \times 10^{-3}$  and  $^{17}\text{O}/^{16}\text{O} = (3.28 \pm 0.23) \times 10^{-4}$ . The presolar grain is in no way related to the nearby CAI.

To determine the elemental composition of the presolar grain, we can use information from the NanoSIMS measurement and the earlier ToF-SIMS

characterization. The NanoSIMS Al data clearly indicate that the  $^{18}\text{O}$ -rich area cannot be an Al-bearing mineral. Since the O intensity is similar to surrounding areas, the presolar grain may be a silicate. To use the ToF-SIMS data for characterization, it is necessary to align the elemental and isotopic images on a sub-micrometer scale. Due to the lack of distinct reference points in the image and the fact that the presolar grain is smaller than the spatial resolution of the ToF-SIMS, this was only partially successful. The area of the presolar grain has a composition that is dominated by O, Fe, Si and smaller amounts of Mg. The presolar grain thus appears to be Fe-rich olivine.

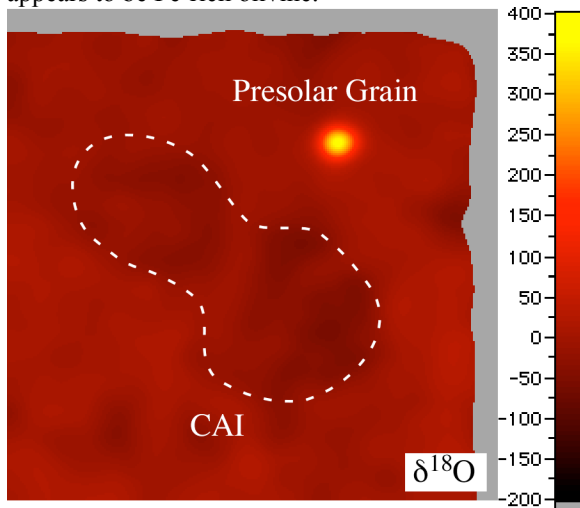


**Figure 2.** False color image of the  $\delta^{18}\text{O}$  distribution in a  $10 \times 10 \mu\text{m}^2$  area of Acfer 094. The approximate outline of a micro-CAI is shown. The composition of the CAI ( $\delta^{18}\text{O} \approx -40\text{‰}$ ) is difficult to discern from the normal background ( $\delta^{18}\text{O} = 0\text{‰}$ ), while the presolar grain stands out as  $^{18}\text{O}$ -rich. The gray area has been excluded from the calculations due to a small image shift.

**Discussion:** The chemical or mineralogical identification of matrix-embedded grains in the sub-micrometer size range is frequently very challenging. In some cases, the transmission electron microscope (TEM) can be used to identify isotopically anomalous mineral phases in focused ion beam (FIB) extracted sections [e.g., 8], but not all samples can be easily extracted. Electron beam X-ray techniques suffer from relatively large excitation volumes and a subsequently low spatial resolution in elemental imaging. A combination of ToF-SIMS and NanoSIMS as demonstrated here can be successful, but requires careful image alignment.

Given the total matrix area analyzed in this study ( $650 \mu\text{m}^2$ ) and the established abundance of presolar silicates in Acfer (176 ppm [4]), it is actually not surprising to find a presolar grain in the analyzed

area. The isotopic composition of the newly found presolar silicate grain is shown in Figure 3 together with those of previously observed silicates in Acfer 094. The new grain is the most  $^{18}\text{O}$ -rich silicate found so far in meteorites, although its O isotopic composition is in the same region (group 4 [9]) of the three-isotope plot as a presolar silicate (pyroxene) found by [3], which is thought to have an AGB star origin. An even more  $^{18}\text{O}$ -enriched silicate grain with a supernova origin was discovered in an interplanetary dust particle [10]. Based on the existing data, both supernovae and asymptotic giant branch (AGB) stars are possible origins for the observed anomaly in the new presolar silicate [9, 11]. The NanoSIMS depth profile data indicate that the presolar grain has not been entirely consumed during the measurement. We can therefore perform additional isotopic measurements (Si, Fe) on the same particle to more closely constrain its origin.

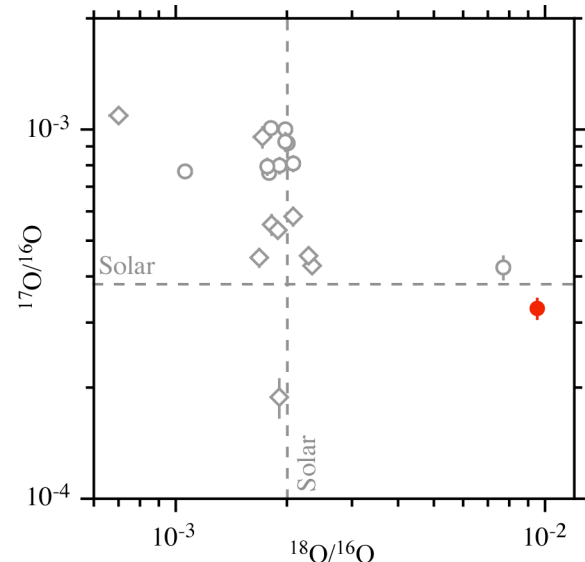


**Figure 3.** Three-isotope plot of the O isotopic compositions of presolar silicates in Acfer 094. The  $^{18}\text{O}$ -rich grain from this study is shown as full red circle. For comparison, the results from previous studies are shown as diamonds [1] and open circles [3]. In most cases, the  $1 \sigma$  error bars are smaller than the symbols.

**References:** [1] Nguyen A. N. and Zinner E. (2004) *Science* 303, 1496-1499. [2] Nagashima K. et al. (2004) *Nature* 428, 921-924. [3] Mostefaoui S. and Hoppe P. (2004) *ApJ*. 613, L149-L152. [4] Nguyen A. N. et al. (2005) *this conference*. [5] Bland P. A. et al. (2005) *this conference*. [6] Stadermann F. J. et al. (2005) *GCA* 69, 177-188. [7] Fagan T. J. et al. (2003) *LPSC XXXIV*, Abstract #1274. [8] Floss C. et al. (2004) *Science* 303, 1355. [9] Nittler L. R. et al. (1997) *ApJ*. 483, 475. [10] Messenger S. and Keller L. P. (2004) *MAPS* 39, A68. [11] Choi B.-G. et al. (1998) *Science* 282, 1284.